Proceedings World Geothermal Congress 2000
Kyushu - Tohoku, Japan, May 28 - June 10, 2000

CHARACTERIZATION OF HDR RESERVOIR BY SEISMIC SIGNAL WHILE DRILLING

Hiroshi Asanuma*, Hakusei Liu*, Hiroaki Niitsuma*, and Roy Baria**
* Graduate School of Engineering, Tohoku University, Aramaki-aza-aoba, Aoba-ku, Sendai 980-8579, Japan
** Socomine, Route-de-Kutzenhausen, Soultz-sous-Forets, F-67250, France

Keywords: seismic while drilling, reflection mehtod, Soultz HDR Project

ABSTRACT

Seismic signals produced while drilling a Hot Dry Rock (HDR) geothermal well in Soultz-sous-Forets, France were detected by two downhole detectors in the granitic basement. Because there was a coherent component arriving at the two seismic stations, the cross-correlation of the signal between the stations was used to estimate the time delay of the direct and reflected phases as well as the autocorrelation of signals from each of the stations. The reflection image by the drill signal was correlated with reflection image by AE reflection method, distribution of microseismicity, and logging data, suggesting that the bottom of the artificial geothermal reservoir and permeable zone inside the reservoir have increased reflection coefficients.

1. INTRODUCTION

In the drilling of HDR wells, on-site, ahead-of the bit detection is effectively used for determination of the drill target. Although this enables us to reduce risk and to improve efficiency associated with HDR development, there are a limited number of techniques available. Vertical seismic profiling (VSP) is one of the most common methods used in practice. However, it is impossible to carry out a VSP simultaneously with drilling and cost considerations prevent frequent VSP measurement during drilling. High temperature and pressure in the basement rock where HDR reservoirs are created also prevents the use of downhole source for reverse VSP's. The seismic while drilling (SWD) technique is another promising means for the real-time detection of the drill target (Asanuma et al., 1991; Rector and Marion, 1991; Haldorsen et al., 1995). Although the signal characteristics are highly dependent on the field and drill system, information about the structure of the earth can be recovered by appropriate signal processing.

A combination of drill bit and downhole multicomponent detectors is one of the best means available for measurement of HDR reservoirs using the drill signal, because the signal is highly attenuated in the overburden and is reflected at overburden/basement boundary. We have been developing the triaxial drill-bit VSP method (TAD-VSP) with a downhole multicomponent detector and have successfully resolved subsurface structures in test sites and geothermal fields to demonstrate its feasibility (Asanuma et. al, 1991; Asanuma and Niitsuma, 1995, 1996).

At the Soutlz HDR site, a HDR well was drilled into basement, and associated drill signals were detected by a multicomponent and two single component seismic detectors both installed in the granitic basement. The authors analysed the multicomponent signals using the principles of the TAD-VSP, and obtained a reflection image around the artificial reservoir which is consistent with logging, the distribution of microseismicity, and results of the AE reflection method (Asanuma et al. 1999). However the TAD-VSP is applicable only to multicomponent signals, and hence the information from single component detector was not used in the previous study despite the requirement to use as much information as possible in downhole measurement when only a limited number of detectors are available.

This paper describes reflection imaging of the Soultz site using multi/single component drill bit signals. After describing the theory to identify reflectors, we discuss the feasibility of the method comparing the drill bit reflection image with other information available at Soultz.

2. BACKGROUND TO THE FIELD

An HDR project has been underway at Soultz-sous-Foret, Alsace, France since 1987 supported by the EC, France, Germany and other organizations (Baria et al., 1995). A view of the Soultz HDR site with locations of wells is shown in Fig. 1. The microseismic data associated with the hydraulic stimulation indicated that there are two zones of rock stimulated, the larger one around a depth of 2900 m, and the smaller one, around 3500 m deep.

A geothermal well, GPK2 (3883 m deep) was drilled in 1994-5. Seismic measurements were taken while roller cone bits of 8" and 6" were being used. Seismic signals at bit depths from 1608 m to 3858 m were detected by one 4-component sensor in well 4550 (depth 1571 m, offset 8 40 m) and by two single component sensors in wells 4616 (depth 1376 m, offset 518 m) and 4601 (depth 1571 m, offset 1253 m). All the sensors were cemented in the granitic basement found below approximately 1300 m.

The seismic signals from sensor in well 4601 had insufficient quality because of the long distance from the bit and unexpected electric noise, and we therefore did not analysed the signal from 4601 in this study. We have previously reported that the signal from 4550 had a relatively white spectra, and that the drill signal is modelled as a point source radiating continuous SV wave dominating over P and SH modes (Asanuma et al., 1996, 1999). The three dimensional hodogram detected by sensor in 4550 was analysed by the triaxial drill-bit VSP (TAD-VSP) and the obtained reflection image was correlated with reflection image by the AE reflection method, the location of microseismicity, logging data and geological information (Asanuma et al., 1996, 1999).

3. COHERENCY OF THE DRILL SIGNAL

To examine the existence of a coherent component in the drill signals which propagated in naturally fractured granite, the coefficients of cross-correlation of the drill signal at sensors in wells 4550 and 4616 were calculated In this analysis, the smoothed coherence transform (SCOT) (Knapp and Carter, 1976) was used to suppress the effect of the dominant frequency component. The coefficient of cross-correlation $C_S(\tau)$ by SCOT is,

$$C_{S,x1x2}(\tau)=F^{-1}\left[W(f)\frac{S^*_{x1}(f)\,S_{x2}(f)}{\sqrt{S_{x1x1}(f)\,S_{x2x2}(f)}}\right] \qquad (1)$$

where $S_{x1}(f)$ is the spectrum of signal $x_1(t)$, $S_{x1x1}(f)$ is the power spectrum of $x_1(t)$, $W(f)$ is the weighting window, * denotes complex conjugate, and operator F^{-1} denotes the inverse Fourier transform.

An example of the power spectral density of signals from wells 4550 and 4616, weighting window and coefficient of correlation are shown in Fig. 2. The calculated arrival time differences of direct P and S waves using a homogeneous velocity in granite are also shown in Fig. 2. It is seen that peaks appear in the correlation coefficient near the expected time delay for direct P and S wave arrivals. The small coefficient suggests that the scattering in the granite is strong. However this nature shows feasibility to detect reflected waves using cross-correlation between signal from two sensors.

4. DISCRIMINATION OF REFLECTED WAVES

The drill signal detected at Soultz has a continuous nature which makes it impossible to directly discriminate reflected waves by observation signals. However, the correlation-based analysis makes it possible to discriminate reflected waves (Asanuma and Niitsuma, 1995, 1999). In this study, because the analyzed drill signals were detected by two sensors, and crosscorrelation analysis can be made as well as autocorrelation analysis. In this study, we used all the possible combination of crosscorrelations and auto-correl ations to extract as much information as possible. These are, (a) autocorrelation of three dimensional hodogram, (b) autocorrelation of single component signal, and (c) cr osscorrelation of signals from two sensors. The concept of the correlation analyses in this study is schematically i llustrated in Fig.3.

Method-(a); autocorrelation of three dimensional hodogr am.
The vector of particle motion, which is detected by a mul ticomponent detector, is a sum of directly arriving and reflected waves which propagate from reflectors at a direction of (φ_i, ψ_i),

$$\begin{aligned}\boldsymbol{o}(nT)=&\boldsymbol{P}(nT)+\boldsymbol{S}(nT-\tau_S)\\&+\sum_{i=1}^{n} k_{P_i}\boldsymbol{A}_i\boldsymbol{P}(nT-\tau_{P_i})\\&+\sum_{i=1}^{n} k_{S_i}\boldsymbol{A}_i\boldsymbol{S}(nT-\tau_{S_i})\end{aligned} \qquad (2)$$

where k: reflection coefficient,
$\boldsymbol{A}$: rotation matrix of (φ, ψ), and
τ: delay relative to directly arriving P wave.

In this study, the term of P waves in (2) can be neglected, assuming small mode conversion at the reflector and the predominant radiation of SV waves from the bit. A motion of SV wave $S(nT, \varphi, \psi)$ from virtual source in direction o f (φ, ψ) is obtained by projecting the vector onto a virtual path (Eq. 3).

$$\begin{aligned}S(nT,\varphi,\psi)=&S(nT)\cos\psi\\&+\sum_{i=1}^{n}\{k_{S_i}S(nT-\tau_{S_i})\sin\varphi_i\sin\varphi\\&+k_{S_i}S(nT-\tau_{S_i})\cos(\psi_i-\psi)\cos\varphi_i\cos\varphi\}\end{aligned} \qquad (3)$$

The crosscorrelation $C(\eta, \varphi, \psi)$, which shows similarity of the SV components from an actual source in a direction of $(0, \psi)$ and a virtual source at (φ, ψ) (Eq. 4), gives extreme at the delay τ_i and propagation direction of reflected waves (φ_i, ψ_i) if signal has spectral whiteness. This technique is used in the TAD-VSP method.

$$C(\eta,\varphi,\psi)=\frac{E[\,S(nT,0,\psi)\,S^*(nT+\eta,\Phi,\psi)\,]}{E[\,S(nT,0,\psi)]^2} \qquad (4)$$

where E[ ] denotes ensemble average.

Method-(b); Autocorrelation analysis of 1C signal.
The autocorrelation of the single component (1C) signal can be used to identify time delay of reflected waves, although estimation of propagation direction is impossible. The 1C signal is written as,

$$Z(nT)=S_Z(nT)+\sum_{i=1}^{n} k_{S_i}S_Z(nT-\tau_{S_i}) \qquad (5)$$

By neglecting terms with power of reflection coefficient k, the autocorrelation function in $\eta > 0$ is,

$$\begin{aligned}C(\eta)=&E[\,Z(nT)\,Z^*(nT+\eta)\,]\\=&\sum_{i=1}^{n} k_{S_i}C_S(\eta-\tau_{S_i})\end{aligned} \qquad (6)$$

This shows that time delay is estimated using autocorrelation for a signal with spectral whiteness.

Method-(c) Crosscorrelation analysis.
Vertical component of signals detected by two sensors are written as,

$$Z_1(nT)=S_Z(nT)+\sum_{i=1}^{n} k_{SI_i} S_Z(nT-\tau_{SI_i}) \quad (7)$$

$$Z_2(nT)=S_Z(nT-\tau_{12})+\sum_{i=1}^{n} k_{S2_i} S_Z(nT-\tau_{S2_i}) \quad (8)$$

Crosscorrelation for $\eta > 0$ between the signals are,

$$C_{12}(\eta)=E[Z_1(nT)\,Z^*_2(nT+\eta)]$$
$$=C_S(\eta-\tau_{12})+\sum_{i=1}^{n} k_{S_i} C_S(\eta-\tau_{S_i}) \quad (9)$$

Eq. 9 shows that the delay of reflected waves between detectors are identified if their delay is larger enough than that of direct waves.

5. REFLECTION IMAGE AT SOULTZ

Migration of the coefficients of auto and cross-correlation onto 3D space was applied using a uniform S-wave velocity. Then, the final reflection image of Soultz was obtained by stacking the three different results. We selected a region where high reflectivity appears in two or three of these three reflection images in order to extract common phenomena in the three different analysis methods.

The deduced distribution of higher reflectivity (k>0.02) is shown in Fig. 4 and 5 comparing with the reflection image by the AE reflection method (Soma et al., 1997a, 1997b) and mapping of microseismic events (Baria et al. ,1995). The depth of higher reflectivity estimated from the drill signal is consistent with that by the AE reflection method at the depths of 3600 m, 3950 m and 4500 m, although these two reflection methods are independent. The reflectivity at 2500 m and 3600 m are possibly the top and bottom of the artificial HDR reservoir, because the cloud of microseismic events with the greatest energy induced during hydraulic fracturing was distributed over this depth interval.

The distribution of reflection coefficients along borehole GPK1 by the drill signal is compared with sonic log, spinner log and borehole televiewer data in Fig. 5. It is seen that the higher reflectivity imaged by the drill bit method around 2800 m depth correlates with a permeable zone at this depth. The velocity of the S wave and acoustic impedance from the sonic log in GPK1 suggests that the physical property of the granite changes near the depths of 3250 m, 3280 m, 3380 m and 3490 m. The acoustic impedance from this method also shows some disturbance at these depths, although the resolution of the TAD-VSP is much lower than of the logging data. It is concluded that the reflectivity imaged by the drill signal is correlated to the distribution of permeable zones, and that localized changes in acoustic impedance are also shown in the drill signal image.

6. CONCLUSIONS

Seismic signals from a drill bit were detected by three downhole detectors in the basement rock during the drilling of an HDR well at Soultz. A reflection image was made by correlation-based analysis of this signal. The estimated subsurface structure correlates well with the reflection image by the AE reflection method and with distribution of microseismic sources suggesting that the upper and lower boundaries of the HDR geothermal reservoir are the predominant reflectors in the granite. Permeable zone and change in the acoustic impedance inside the reservoir were also detected by this method.

The combination of microseismicity and drill signal is one of the best ways to measure the internal structure of deep engineered geothermal reservoirs. As the reservoir extension is not directly estimated from the distribution of microseismicity, the drill signal will be effectively used to image the reservoir boundary and pre-existing permeable zones which have low seismic efficiency.

ACKNOWLEDGEMENTS

The work described in this paper was carried out as a part of MURPHY/MTC International Collaborative Project which are supported by NEDO (International Joint Grant). We would also like to thank Socomine for providing the data from the European HDR site at Soultz which is supported mainly by the European community, BMBF (Germany) and ADEME (France).

REFERENCES

Asanuma, H., Niitsuma, H., and Chubachi, N., 1990, An analysis of three dimensional AE Lissajou pattern and estimation of source direction, Prog. Acoust. Emiss., 5, 436-443.

Asanuma, H., and Niitsuma, H., 1995, Triaxial seismic measurement while drilling and estimation of subsurface structure, Geotherm. Sci. Tech., 5, 31-51.

Asanuma, H., Park, J.N., Niitsuma, H., and Baria, R., 1996, Characterization of subsurface structure at Soultz-sous-Forets (France) by triaxial drill-bit VSP, 66th Ann. Interna t. Mtg. SEG, 202-205.

Asanuma, H., Liu, H., Niitsuma, H., and Baria, R., 1999, Identification of structures inside basement at Soultz-sous-Foret (France) by the triaxial drill-bit VSP, Geothermics (in press)

Baria, R., Garnish, J., Baumgartner, J., Gerad, A., and Jung, R., 1995, Recent developments in the European HDR research programme at Soults-sous-Forets (France), Proc. World Geotherm. Cong., 2631-2637.

Haldorsen, J. B. U., Miller, D.E., and Walsh, J.J., 1995, Walk-away VSP using drill noise as a source, Geophysics, 60, 978-997.

Knapp, C.H., and Carter, G.C., 1976, The generalized correlation method for estimation of time delay, IEEE Trans.Acoust., Speech, Sig. Process., 4, 320-327.

Rector, J. W., and Marion, B.P., 1991, The use of drill-bit energy as a downhole seismic source, Geophysics, 56, 628-634.

Soma, N. and Niitsuma, H., 1997a, Identification of structures within the deep geothermal reservoir of the Kakkon

da Field, Japan by a reflection method using acoustic emi ssion as a wave source, Geothermic 26, 43-64.

Soma, N., Niitsuma, H., and Baria, R., 1997b Estimation of deeper structure at the Soultz Hot Dry Rock Field by means of reflection method using 3C AE as wave source, PAGEOPH 150, 661-676.

White, J.E., 1965, Seismic waves: Radiation, transmission, and attenuation, McGraw-Hill Book Co.

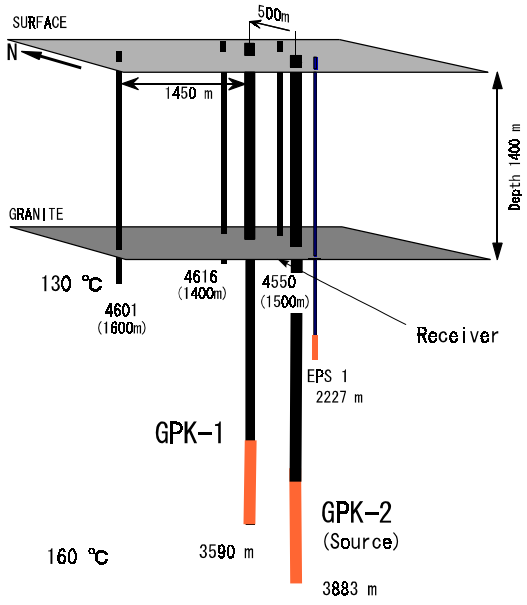

Fig. 1 A view of the Soultz HDR Field.

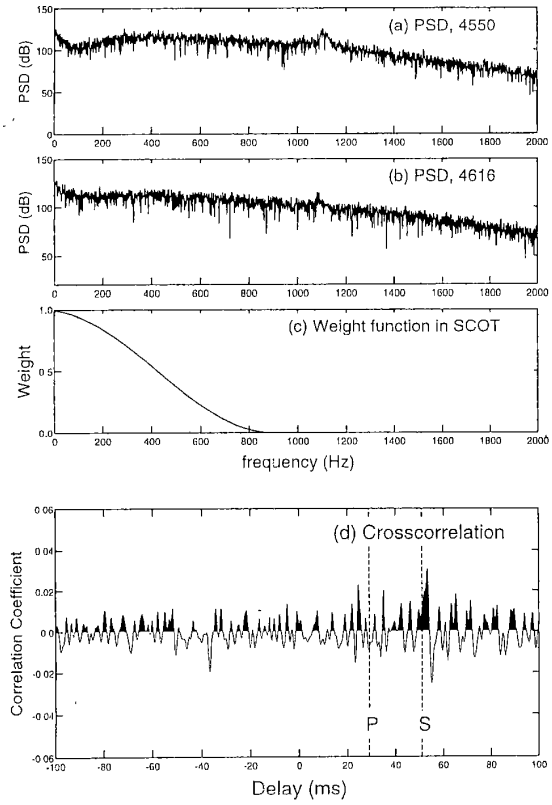

Fig. 2 Power spectral density of the drill signal from 4550 and 4616, weight function and coefficient of cross correlation between 4550 and 4616.

Method-(a); Autocorrelation analysis of hodogram

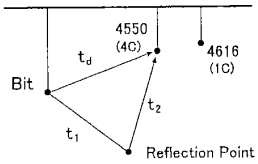

Method-(b); Autocorrelation analysis of 1C signal

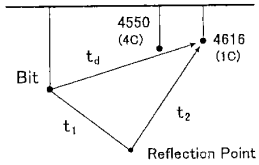

Method-(c); Crosscorrelation analysis

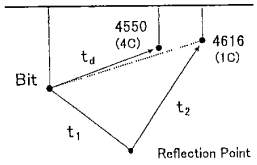

Fig. 3 Concept of the correlation analyses to discriminate reflected waves.

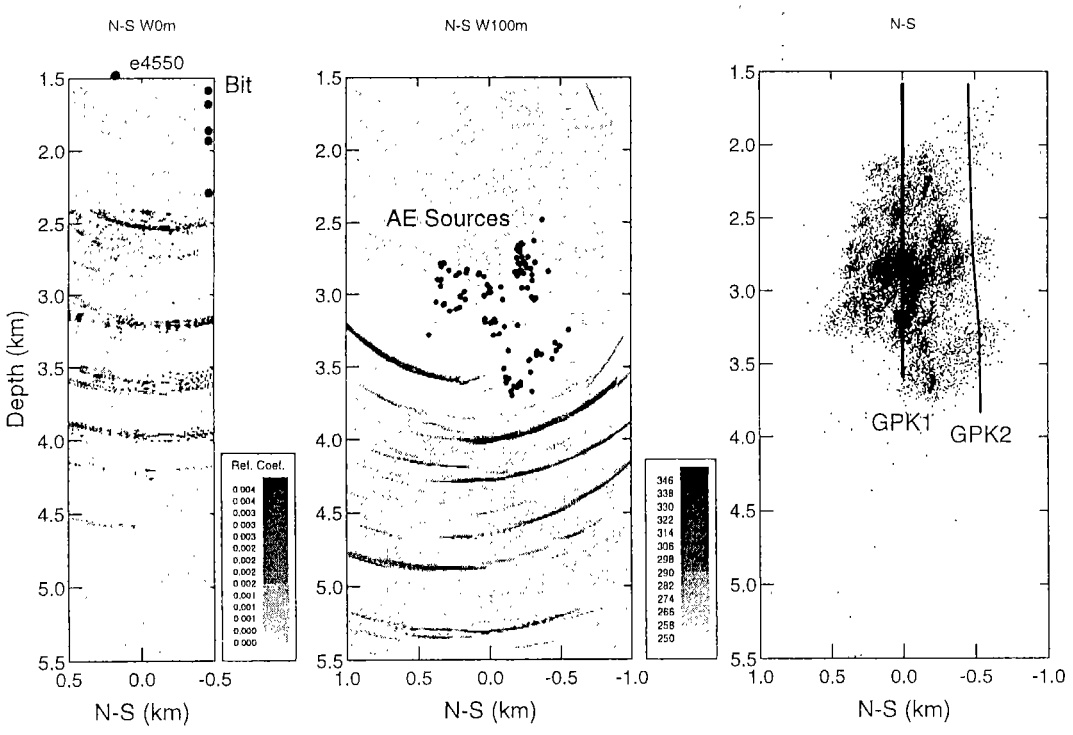

Fig. 4 Distribution of reflection coefficients estimated from the drill signal. Distribution of reflectivity by the AE reflection method and location of microseismic events during stimulation in 1993 are also shown

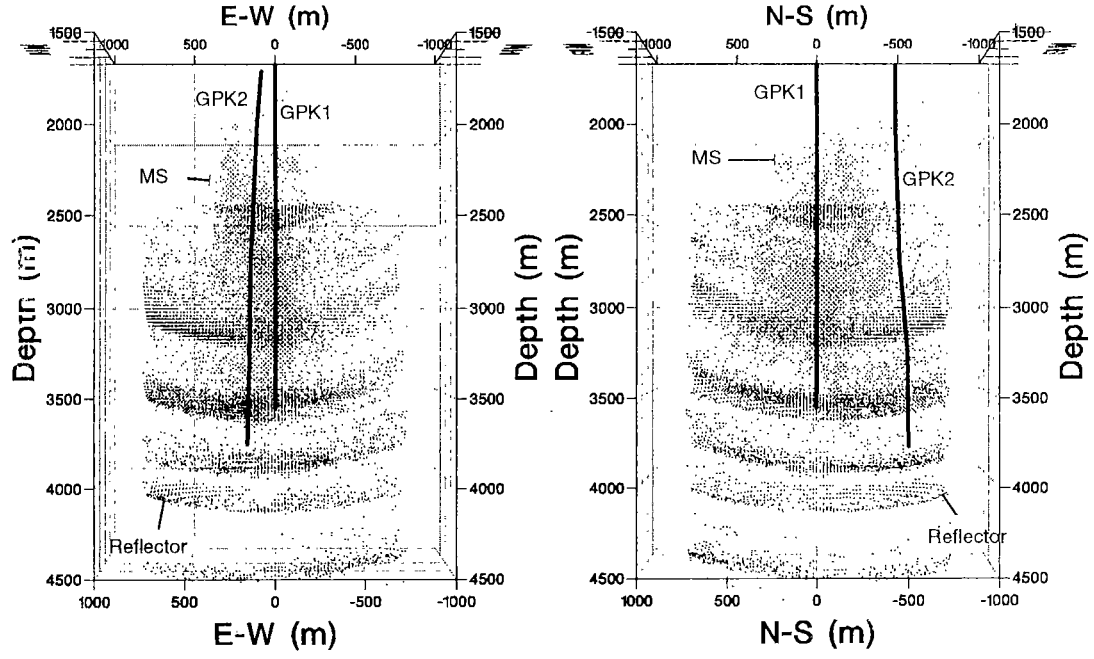

Fig. 5 Three dimensional distribution of reflectivity estimated from drill signal. Location of microseismicity during stimulation are also shown.

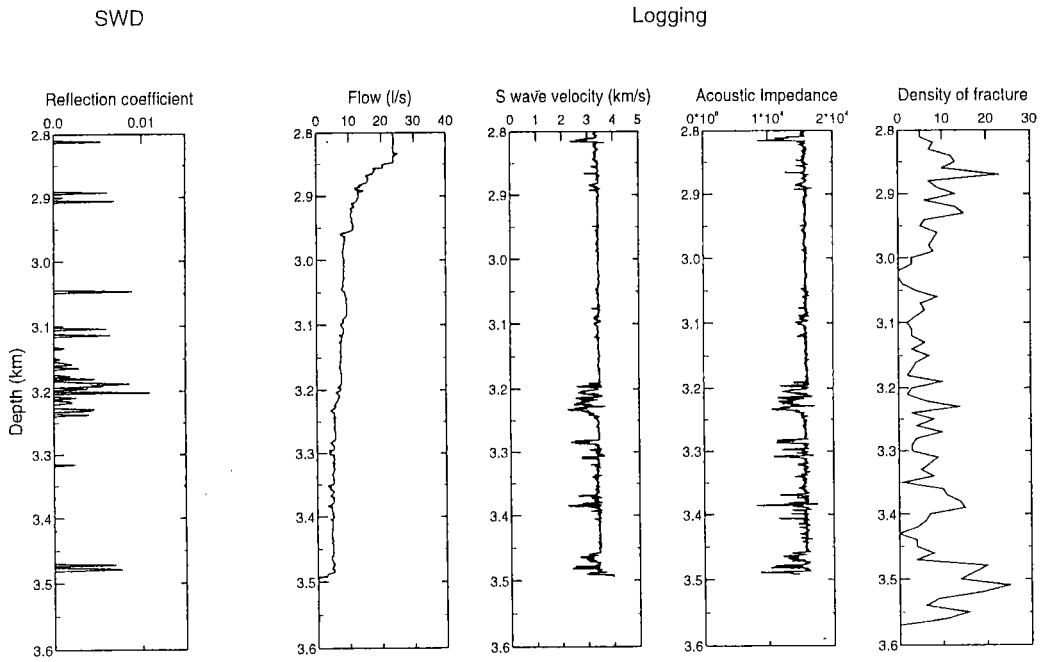

Fig. 6 Comparison of reflection coefficient and change in acoustic impedance, sonic log, spinner log and fracture distribution by BHTV.